

**HYDROLOGIC MODELING IN WATERSHEDS OF THE EASTERN PALOUSE:
ESTIMATION OF SUBSURFACE FLOW CONTRIBUTIONS**

E.S. Brooks, P.A. McDaniel, and J. Boll

Presented at the 2000 PNW-ASAE Regional Meeting, Sept 21-23, Paper 2000-10, ASAE, 2950
Niles Road, St. Joseph, Michigan 49085-9659, USA

INTRODUCTION

Throughout the Pacific Northwest there has been an increasing awareness of the impact of point and non-point source pollution on stream and lake water quality. In Idaho over 900 streams have been listed on the 303(d) list for exceeding the total maximum daily loads as defined by the Clean Water act for a number of pollutants, including suspended sediment, phosphorous and water temperature. In order to decrease pollutant loading to acceptable levels, each stream or lake segment has been assigned a Watershed Advisory Group (WAG) who is responsible for developing a watershed implementation or management plan. The challenge in developing these plans is determining which areas in the watershed should receive the greatest amount of restoration to bring about the largest decrease in loading. Due to limited time allowances to properly monitor the problem, WAG's must rely on general observations or computer modeling to assist in decision making.

Distributed hydrologic modeling in geographic information systems (GIS) has shown promise as a tool watershed managers can use to identify spatially within a watershed the location of runoff generating areas (Boll et al., 1998; Frankenberger et al., 1999). However, there are some obvious disadvantages to computer modeling. Typically models require an excessive number of input parameters not readily available in a watershed database, they operate at a coarse spatial or temporal scale, they require excessive calibration, or they are not based on the dominant hydrologic processes in the watershed. A model must predict surface runoff with acceptable accuracy before considering erosion or nutrient modeling. Calibration and data collection should be limited if watershed managers are to use hydrologic models.

This project focuses on characterizing and quantifying the dominant hydrologic processes of the Northwest Wheat and Range Region (NWRR) to develop a distributed hydrologic model specific for the NWRR. The NWRR is characterized by low intensity rainfall which falls on wind deposited loess soils. Excessive erosion is accelerated by large rain on snow events that are enhanced by seasonal frozen soil. Most of the soils in the region have shallow buried paleosols or fragipans that have limited vertical water flow. As a result seasonal perched water tables can cause saturation excess runoff. Due to the low intensity rainfall, little infiltration excess or Hortonian runoff occurs except on bare fallow fields that have surface sealing or crusting. The loess soils were deposited on long, steep slopes in a dune-like manner that can lead to large lateral subsurface water flow contributing to saturation excess or variable source area runoff.

Boll et al. (1998) showed that a modified version of the Soil Moisture Routing (SMR) model (Frankenberger et al., 1999) could predict with reasonable accuracy the perched water table fluctuations in a 2 ha watershed in the NWRR. The model is being modified and developed for the climatic and hydrologic conditions of the NWRR under the constraints of relying on little or no calibration and using publicly available data. Boll et al. (1998) showed that the key parameters in the model for this region are the lateral saturated hydraulic conductivity (K_{sat}) of the topsoil and the vertical hydraulic conductivity of the fragipan. It was hypothesized that the lateral K_{sat} was larger than the K_{sat} value reported in the county soil survey due to preferential flow through cracks and large pores. The hypothesis was supported by a small tracer study conducted during perched water conditions in the NWRR where we detected bromide moving 7 m to a tile line in 9 hours. The effect of macro-pores on lateral flow has been extensively documented in forest soils and well developed structured soils (Beven and German, 1982). However there is limited literature on large lateral flow for soils used in agricultural production.

The objectives of this paper are to 1.) quantify the lateral subsurface flow that occurs over a soil having a hydraulically restrictive fragipan subsurface layer, 2.) determine and compare the lateral K_{sat} to the K_{sat} reported in the soil survey and 3.) resolve the vertical percolation rate through the fragipan layer using a water balance. An isolated hillslope plot was used to measure the lateral subsurface flow and a water balance was used to determine the percolation rate through the fragipan.

MATERIALS AND METHODS

Site Description

The research site is located 5 miles north of Troy, ID in the Eastern portion of the NWRR (SE $\frac{1}{4}$, SE $\frac{1}{4}$, S35, T.40N., R.4W) in a field having undisturbed perennial grasses as a part of the Conservation Reserve Program. The site experiences perched water table due to a fragipan located at ~ 0.65 m. As described by Boll et al. (1998), the Latah County soil survey (Barker, 1971) identifies the soil type as a Santa Series, which consist of moderately well-drained soils with a moderately deep profile extending to a fragipan. The taxonomic class is coarse-silty, mixed, frigid Ochreptic Fragixeralfs. The profile contains three genetic horizons, A, Bw¹, E, and a fragipan, Btxb. The A horizon is a yellowish brown silt loam that is dark brown when moist with a subangular blocky structure that is 0 to 38 cm deep. The Bw horizon is a brown silt loam with a prismatic structure and is 38 to 68 cm deep. The E horizon is a pale brown silt loam with a massive structure that is slightly hard and is 68 to 86 cm deep. The Btxb horizon, or fragipan, is a yellowish brown silt loam and silty clay loam soil with a coarse prismatic and medium angular blocky structure that is very hard, firm, and brittle and ranges from 86 to 165 cm deep. The mean annual precipitation for the eastern Palouse ranges from 500 mm in the west to over 830 mm in the east. More than 60% of the annual precipitation occurs from November to April with low intensity rainfall or snowmelt. Soils at the site did not freeze during the testing period due to the insulating effect of a snow cover.

Soil hydraulic properties, including field capacity, bulk density, and porosity were measured directly in the plot using replicated ~ 5 cm diameter soil cores. The thickness of each soil horizon was visually documented when installing the wells. The topography was measured with a detailed site survey.

Plot Design

A hillslope plot (~ 30 m x 18 m) having a slope of $\sim 20\%$ and an aspect of 345° from due north was isolated using tile lines and plastic sheeting. The size of the plot was selected to represent the typical mapping unit (30 m x 30 m) in GIS modeling applications. As seen in Figure 1, an upslope tile line was installed on the fragipan to divert incoming lateral subsurface flow and a downslope tile line was installed to collect and divert the outgoing lateral flow to an automated tipping bucket flow measuring device. A datalogger recorded the flow rate every 15 minutes. All sides of the plot were lined with plastic sheeting and incoming surface runoff was diverted using galvanized sheet metal borders. Outgoing surface runoff was measured using a trough draining to a similar tipping bucket flow gage.

¹ For ease of use in variables B is substituted for Bw in the remainder of the text

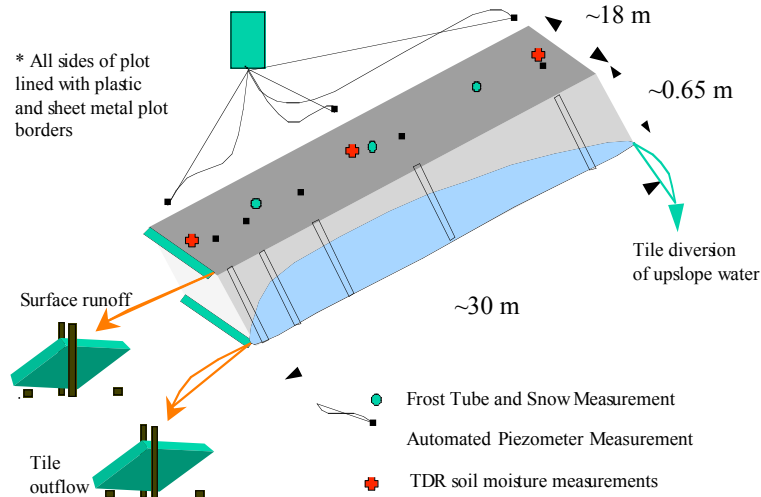


Figure 1 Hillslope plot layout and instrumentation.

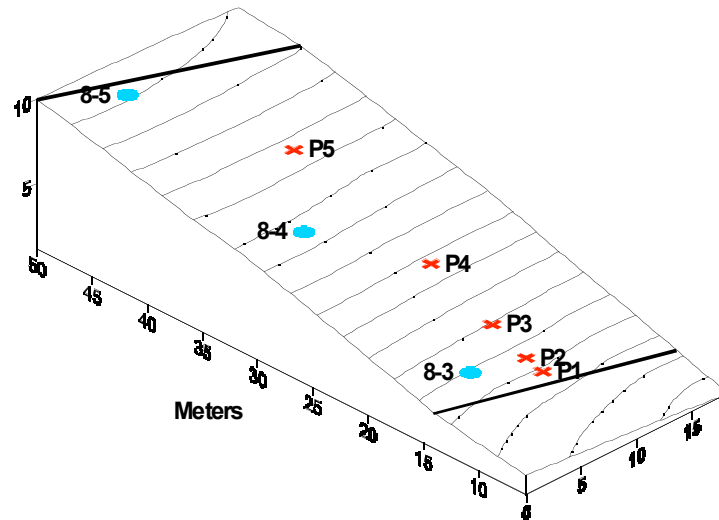


Figure 2 Contour map of the site. Wells identified with a circle were read every 12 hours. Wells identified with a cross were read every site visit.

The plot consisted of three shallow wells extending down to the fragipan. Each well was equipped a pressure transducer that was read every 12 hours using a Campbell Scientific CR10x datalogger (Figure 2). The shape of the draw down curve to the tile line was monitored manually with every site visit (~ weekly) using 5 wells spaced at distances of 0.5, 2.0, 4.9, 10.9, and 22.8 m uphill from the lower tile line (see Figure 2). Snow water equivalent depth was measured with every site visit. A weather station located at the site recorded hourly temperature, relative humidity, wind speed, solar radiation, soil temperature, and precipitation. Soil moisture content was measured every 15 cm down to a depth of 75 cm vertical Moisture Point® sensors based on time domain reflectometry (TDR) developed by Environmental Sensors Inc. (ESI). Moisture measurements were taken only during site visits.

Drainage of Sloping Land

Tile drains installed on sloping land are referred to as interceptor drains. Interceptor drains are used to reduce the saturation excess runoff downslope of the drain. Childs (1971) presented a solution to groundwater flow to a ditch or tile line over a sloping impermeable bed. Assuming flow lines are approximately parallel to the bed, according to the Dupuit-Forchheimer approximation, then, by means of Darcy's law, the flow of water per unit width to the drain can be written in terms of the lateral K_{sat} and the absolute slope of the water table. This conceptual model is shown in Figure 3. The bed slope is at an angle α , the thickness of the saturated layer over the bed is T , and the distance along the bed is defined as s .

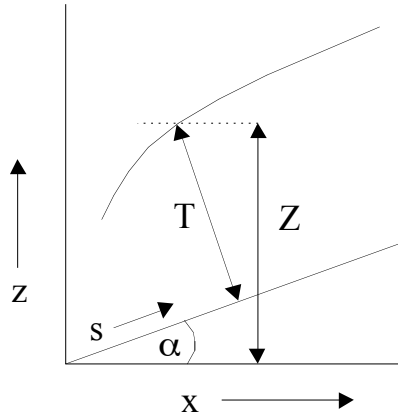


Figure 3. Conceptual model of lateral saturated flow to a tile (Childs, 1971).

By letting x be an arbitrary datum level and Z the distance from the datum level to the water table, then the flow to the tile or ditch (q) can be written as:

$$q = -K_{sat}T \left(\frac{dZ}{ds} \right) = -K_{sat}T \left(\frac{dT}{ds} \cos \alpha + \sin \alpha \right) \quad (1)$$

In the present study, q , T , and the slope of the water table were measured directly, so that equation (1) can be solved directly for the lateral K_{sat} .

Vertical Percolation

Vertical percolation of water into the fragipan was estimated using a mass balance for the hillslope plot. This mass balance can be written as:

$$D \frac{d\theta}{dt} = Rain + Snowmelt - Q_{lat} - Perc - ET \quad (2)$$

where D is the soil thickness above the fragipan, θ is the soil water content, t is time, Q_{lat} is the lateral flow leaving the plot as tile flow, $Perc$ is the vertical percolation rate through the fragipan and ET is the amount of water that leaves the plot through evapotranspiration. Rain and snowmelt were calculated simultaneously using a daily snowmelt energy balance model based on the work of Walter (1995) and the Army Corps of Engineers (1960). The potential ET for a grass crop was calculated daily using the Penman Montith equation as programmed in the Ref-

ET model of Allen (2000). Actual ET was related to potential ET using crop coefficients. The crop coefficients were set by analyzing periods of time when the perched water table had receded and soil moisture measurements were available. During this time the only percolation which occurs is through unsaturated flow which can be assumed to be negligible through the fragipan. Therefore the water balance can be solved for actual ET. Crop coefficients were fixed at 0.25 for the first 20 days with positive heating degree days, and increased to 1.0 over the next 30 days following the procedure of Doorenbos and Pruitt (1977). Percolation was determined on a daily basis from all other components of the water balance. The change in soil water content with time was quantified by periodic manual soil moisture measurements and by relating the soil water content to the depth to water table, as discussed in the following section.

RESULTS AND DISCUSSION

In this section we describe how we quantified each component of the mass balance. It is essential that all components be measured or predicted accurately. We quantify the error in snowmelt modeling. With a good estimate for snowmelt we can quantify the total lateral flow as it relates to the addition of rain and snowmelt. From the measured lateral we calculate the lateral K_{sat} . In order to quantify the change in soil storage we evaluate a method for determining the soil water content using depth to water table. Finally when all components of the water balance are considered we estimate the percolation through the fragipan by analyzing the cumulative error in the mass balance.

Measured Soil Hydraulic Properties

The change in soil porosity with depth was calculated from bulk density measurements on soil cores taken from the plot assuming a particle size density of 2.65 g cm^{-3} . Twenty soil cores were taken with depth from the plot. Equation 3 is the best fit straight line through the data points.

$$\phi = 0.0022z + 0.360 \quad R^2 = 0.59 \quad (3)$$

The porosity (ϕ) increases linearly from 36.0% at the fragipan ($z = 0$) to 50% at the soil surface at well (8,3) ($z = 64$). The coefficient of determination (R^2) for the linear fit was 0.59.

The samples were taken on 12/6/99, just prior to the establishment of a perched water table on the fragipan. The volumetric moisture content (θ) using these same samples also followed a roughly linear relation as described by equation (4).

$$\theta = 0.0008z + 0.350 \quad R^2 = 0.42 \quad (4)$$

Equation (3) and (4) indicates that at the fragipan ($z = 0$) the difference between the moisture content and the porosity is 1%. Since very little additional rainfall caused a perched layer to form after these samples were taken then equation (4) can be used as a good approximation for the change in field capacity with depth. The large values for field capacity for these soils explains the successful dryland wheat and pea production in the NWRR.

Measured Components of the Mass Balance

Change in soil water storage was determined from soil moisture measurements coupled with the change in water table heights measured in the wells. In the presence of a water table, the

change in soil water storage is commonly referred to as the drainable porosity. Drainable porosity is defined as the volume fraction of pore space that can be drained from a soil during a water table draw down. Taylor (1960) showed that the drainable porosity is related to soil type and the depth to a free water surface. Using the data used to develop equations (3) and (4) and manual soil moisture measurements with the Moisture Point sensors throughout the year the following relationship was developed to relate the drainable porosity (f) in cm^3/cm^3 to depth to the water table ($D - h$), see Figure 4.

$$f = 0.00096(D - h) \quad (5)$$

As seen from equation (5) a 100 cm drop in the water table is associated with a 9.6% drop in total soil moisture. Average drainable porosity, or sometimes called specific yield, ranges from 2% in clay soils to 15% in sand soils (Taylor, 1960, Troch et al., 1993, U.S.B.R., 1993). With equation (5) and the function relating the total porosity with depth, the total depth of water stored in a soil column (S) can be estimated at any time there is a water table present with the following equation.

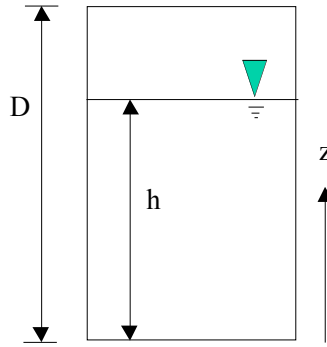


Figure 4. Single partially saturated soil column.

$$S = \phi(z) - f(z) = \int_0^D 0.0022z + 0.3597 dz - \int_0^{D-h} 0.00096z dz \quad (6)$$

In equation (6), D is defined as the total soil thickness and h is the thickness of the perched water table, see Figure 4.

Integrating (6) results in the following function for the depth of water in a soil column.

$$S = \frac{0.0022}{2} D^2 + 0.3597D - \frac{0.00096}{2} (D - h)^2 \quad (7)$$

As seen in Table 1, the percent error between predicted and measured depth of soil water is less than $\pm 5\%$. The accuracy of this method cannot be fully tested without more measured points.

Table 1. Comparison between measured and predicted total water storage amount.

Date	Location	Soil Depth (cm)	Perched Water Table Thickness (cm)	Measured Depth of Soil Water (cm)	Predicted Depth of Soil Water (cm)	Percent Error
4/10/00	(7,4)	60	7.5	24.5	23.9	-2.4%
4/20/00	(7,4)	60	15.3	24.9	24.0	-3.6%
5/15/00	(7,4)	60	14.7	25.0	24.0	-4.1%
4/10/00	(8,3)	64	5.8	25.4	25.6	0.9%
4/20/00	(8,3)	64	14.9	26.0	25.7	-1.2%
5/15/00	(8,3)	64	2.9	26.2	25.6	-2.3%
4/10/00	(8,5)	61	0.0 ¹	23.9	24.3	1.6%
4/20/00	(8,5)	61	0.0 ¹	24.2	24.3	0.3%

¹The water table had just recently receded to 0 cm.

Snowmelt

Figure 5 shows predicted and observed snow water equivalent using a daily energy balance snowmelt model based on the work of Walter (1995) and the U.S. Army Corps of Engineers (1960). The root mean square error between the measured and predicted points is 1.2 cm. The small error between predicted and observed values was produced with little calibration.

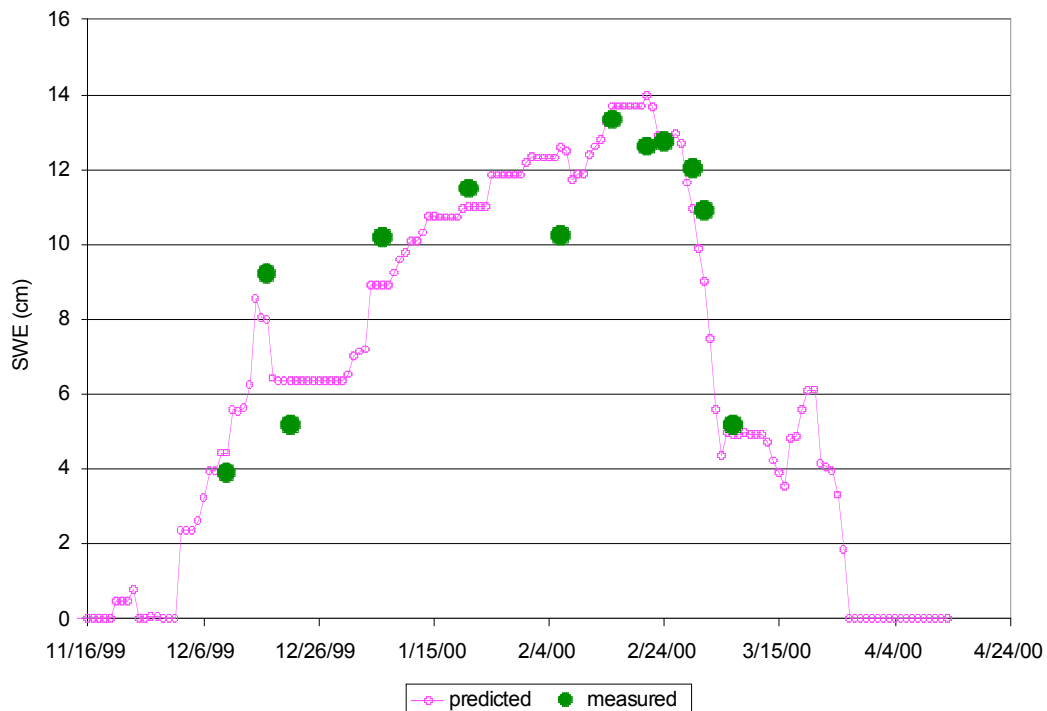


Figure 5. Measured and predicted snow water equivalent at the hillslope plot.

Lateral Subsurface Flow

Figure 6 shows the lateral tile flow and the input rain and snowmelt predicted using the energy balance snowmelt model. For the time period that the tile line was recording data

(2/16/200 - 5/17/2000), 88.6% of the total precipitation left the plot as lateral flow. We did not measure any significant runoff from the plot throughout the study.

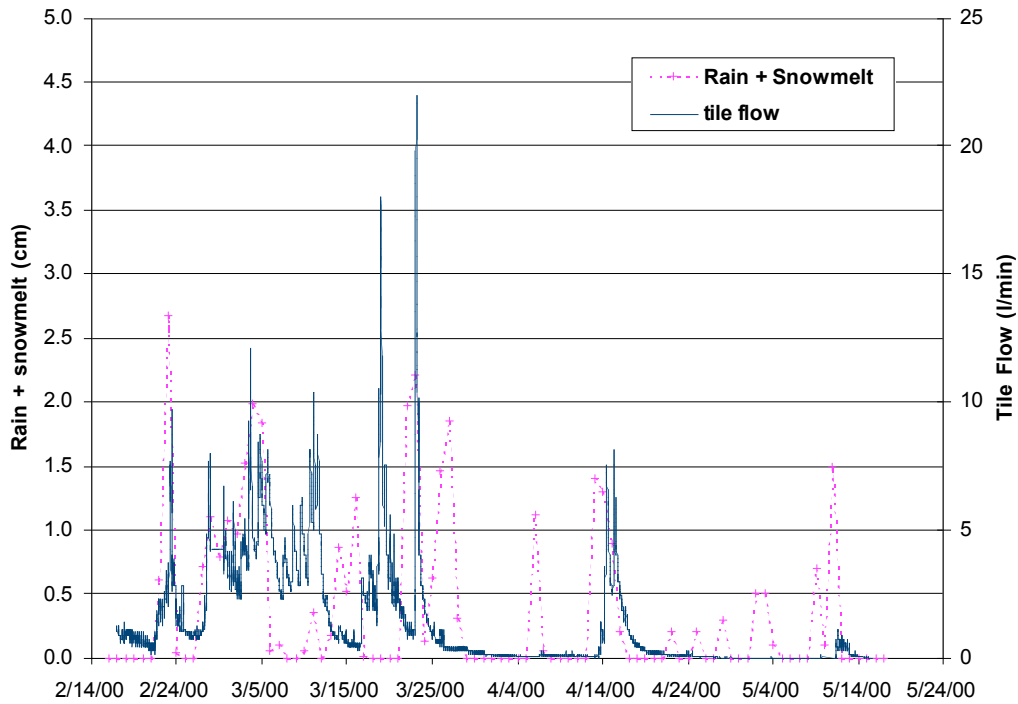


Figure 6. Measured tile outflow and predicted snowmelt.

Lateral Saturated Hydraulic Conductivity

The lateral K_{sat} was predicted daily using equation (1). The lateral flow (q) was measured with the tipping bucket flow gage, the thickness of the saturated layer (T) was measured at well 8-3 (see Figure 2), and the slope of the water table was determined from well measurements at 8-3 and 8-4. Manual measurements showed that the slope of the water table was nearly equal the land slope near the downslope border of the plot.

Figure 7 shows the predicted effective lateral K_{sat} for different depths of perched water at the tile outlet. It is identified as the “effective” lateral K_{sat} since it is the K_{sat} determined over the entire depth of the water table not specifically for each soil layer. As seen in Figure 7 the effective lateral K_{sat} decreases exponentially from the soil surface to the fragipan. Beven (1982) uses this same exponential trend in TOPMODEL. An exponential fit to all the data shows an under prediction of the effective conductivity in the A-Horizon. A separate fit to the A-Horizon data better represents the trend in the data.

The actual average lateral K_{sat} for each soil layer was determined through integration of the exponential relationship given in Figure 7. These actual lateral K_{sat} values for each layer are displayed in Table 2. Also listed in Table 2 are vertical K_{sat} values reported by Young (1998) that were determined from 8 cm diameter soil cores taken from the A, B, and E horizons, and the average vertical K_{sat} value reported in the Latah County soil survey (Barker, 1981) for the entire top soil thickness.

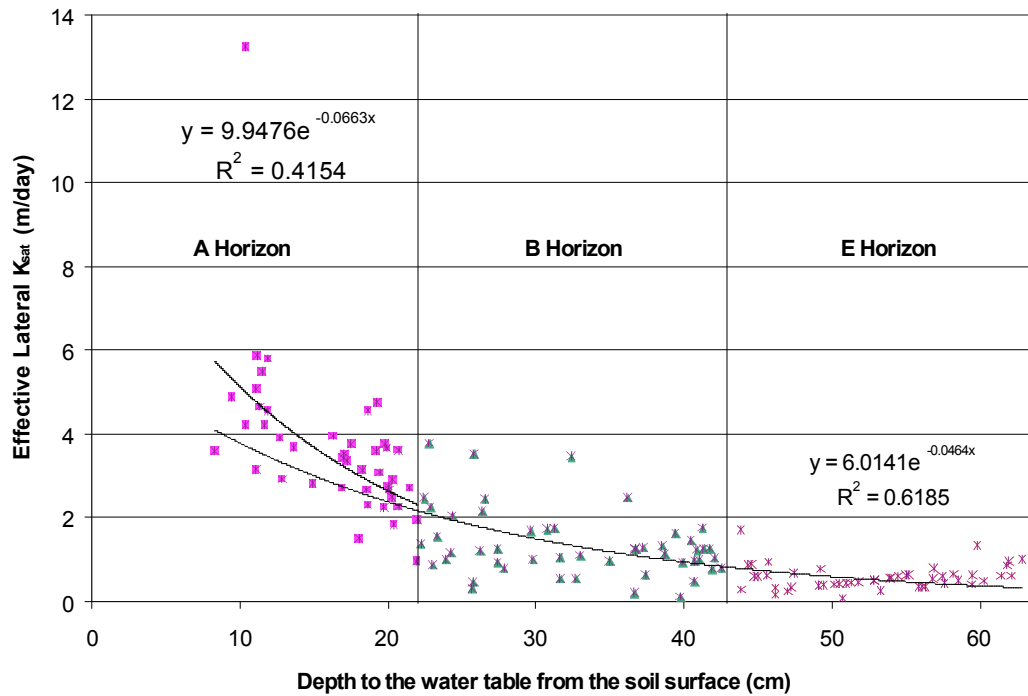


Figure 7. Predicted effective lateral K_{sat} with depth to water table.

As seen in Table 2 the lateral K_{sat} measurements are, on average, three times larger than the vertical K_{sat} measurements reported by Young (1998) and Barker (1981). The largest discrepancy between the lateral and vertical K_{sat} measurements occurs in the A horizon.

Table 2. Lateral versus vertical K_{sat}

Soil Horizon	Hillslope Plot Lateral K_{sat} m/day	Young (1998) Vertical K_{sat} m/day	Ratio of lateral to Young (1998) vertical K_{sat}	Soil Survey Vertical K_{sat} m/day	Ratio of lateral to Soil Survey vertical K_{sat}
A	13.4	1.6	8.4	NA ¹	NA ¹
B	2.4	0.5	4.8	NA ¹	NA ¹
E	0.5	0.2	2.7	NA ¹	NA ¹
A+B+E	5.4	0.8	7.1	0.8	7.1

¹The latah county soil survey treats the A, B, and E soil horizons as one soil layer

Percolation through the fragipan

Figure 8 shows the cumulative error in the water balance throughout the year for percolation rates of 0, 0.01, and 0.1 cm/day. The cumulative error is defined by the following equation.

$$error = Rain_t + Snowmelt_t - Q_{lat,t} - Perc_t - ET_t - D(\theta_{(t)} - \theta_{(t-1)}) \quad (8)$$

In Figure 8 a positive error indicates the input to the plot, rain + snowmelt, was greater than the output from the plot and the change in storage within the plot.

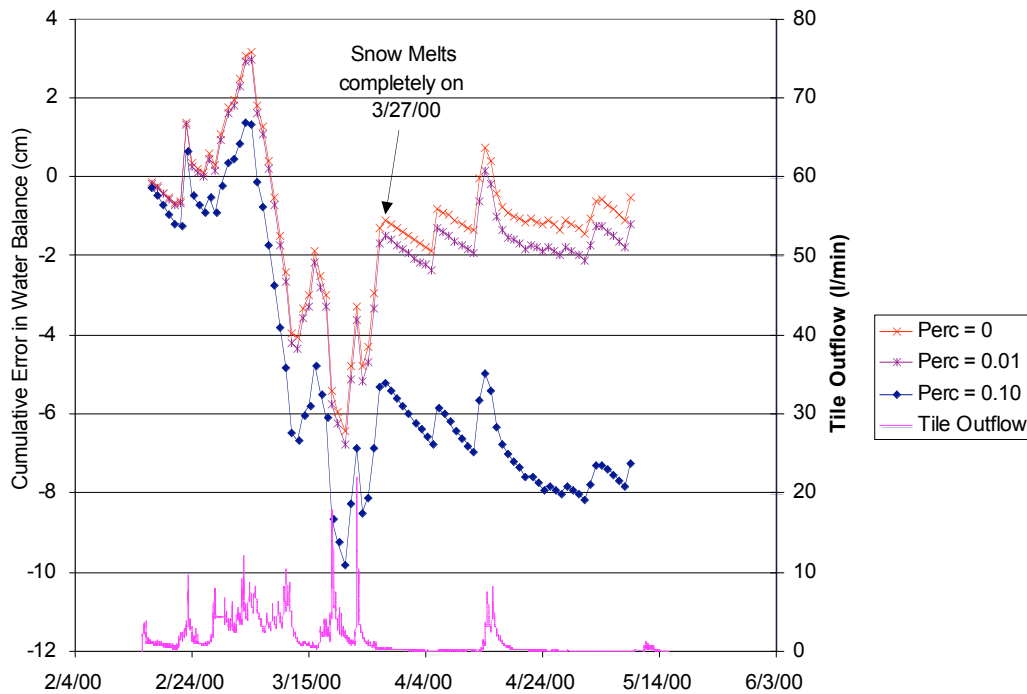


Figure 8. The cumulative error in the water balance for percolation rates of 0, 0.01, and 0.10 cm/day.

If all components of the water balance were predicted accurately the cumulative error would be zero. As seen in Figure 8 the cumulative error initially starts with a positive error and then drops significantly. By 3/27/00 the error close to zero (~ -1 cm). Since 3/27/00 corresponds to the day when the snow completely melted on the plot, these initial fluctuations are most likely due to errors in the timing of predicted snowmelt.

Since the cumulative error significantly decreases with a percolation rate of 0.1 cm/day then an estimate of 0 to 0.01 cm/day is most likely closer to the actual percolation rate. Without measuring E_t and precipitation more accurately the precise value for percolation cannot be measured.

CONCLUSION

The eastern half of the NWRR is characterized by hydraulically restrictive soil layers that lead to seasonally perched water tables. Since the region has long steep slopes lateral subsurface flow can be significant. In this study 88% of the total precipitation left a 18 x 30 m hillslope plot having a fragipan at ~ 65 cm as subsurface lateral flow. The lateral K_{sat} decreased exponentially from 13.4 m/day and the soil surface to less than 0.5 m/day near the fragipan. These measurements of lateral K_{sat} were on average 7 times larger than vertical K_{sat} measured on 8 cm diameter soil cores and 7 times larger than the vertical K_{sat} indicated in the soil survey. A mass balance on the plot indicated that the vertical percolation rate through the fragipan layer is on the order of 0 to 0.01 cm/day.

These findings indicate that the hydrology of the region is dominated by subsurface lateral flow that is the main driving force in the generation of variable source area saturation excess

runoff. The measurement of the lateral K_{sat} and the percolation rate through a fragipan soil will reduce the calibration required in distributed hydrologic models developed for this region.

REFERENCES

- Allan, R.G. 1999. REF-ET Reference evapotranspiration software. <http://www.kimberly.uidaho.edu/REF-ET/>, Kimberly Research and Extension Center, University of Idaho, Kimberly, ID.
- Barker, R.J. 1981. *Soil survey of Latah County area, Idaho*. U.S. Dept. of Agriculture, Soil Conservation Service, 166pp.
- Bevan, K. and P. Germann. 1982. Macropores and water flow in soils. *Water Resources Research*, 18(5):1311-1325.
- Beven, K.J. 1982. On subsurface stormflow: An analysis of response times, *Hydrol. Sci. J.*, 27:505-521.
- Boll, J., E.S. Brooks, C.R. Campbell, C.O. Stockle, S.K. Young, J.E. Hammel, and P.A. McDaniel. 1998. Progress toward development of a GIS based water quality management tool for small rural watersheds: modification and application of a distributed model. Presented at the 1998 ASAE Annual International Meeting in Orlando, Florida, July 12-16, Paper 982230, ASAE, 2950 Niles Road, St. Joseph, MI 49085-9659, USA.
- Childs, E.C. 1971. Drainage of groundwater resting on a sloping bed. *Water Resources Research*, 7(5):1256-1263.
- Doorenbos, J. and W.O. Pruitt. 1977. Guideline for predicting crop water requirements. *FAO Irrig. Drain. Paper No. 24*:1-144.
- Frankenberger, J.R., E.S. Brooks, M.T. Walter, M.F. Walter, T.S. Steenhuis. 1999. A GIS-based variable source area hydrology model. *Hydrologic Processes*, 13:805-822.
- Taylor, G.S. 1960. Drainable porosity evaluation from outflow measurements and its use in drawdown equations. *Soil Science*, 90(6):338-343.
- Troch, P.A., F.P. De Troch, and W. Brutsaert. 1993. Effective water table depth to describe initial conditions prior to storm rainfall in humid regions. *Water Resour. Res.*, 29(2):427-434.
- U.S. Army Corps of Engineers. 1960. Engineering and Design: Runoff from Snowmelt. EM 1110-2-1406.
- U.S. Bureau of Reclamation. 1993. Drainage Manual, A water resources technical publication. U.S. Department of the Interior, pp. 321.
- Walter, M.T. 1995. Winter-time hydrologic modeling over a three dimensional landscape. Unpublished Ph.D. dissertation, Washington State University, Pullman, WA.
- Young, S.K. 1998. Soil hydrology in an eastern Palouse micro-catchment underlain by a fragipan. Unpublished M.S. thesis, University of Idaho, Moscow, ID.